RSC Advances

PAPER

View Article Online
View Journal | View Issue

Cite this: *RSC Adv.*, 2025, **15**, 12547

Light-driven CO_2 reduction with substituted imidazole-pyridine Re catalysts favoring formic acid production†

Ryan Chafin,‡[a] Majharul Islam Sujan, ‡[b] Sean Parkin, [a] Jonah W. Jurss [b] and Aron J. Huckaba *[a]

Removing carbon dioxide from the atmosphere is an attractive way to mitigate the greenhouse gas effect that contributes to climate change. A series of donor-pi (D-π), acceptor-pi (A-π), and π Re(I) pyridyl imidazole complexes have been synthesized and examined under photocatalytic conditions for the photocatalytic reduction of CO_2. The catalytic activity of the complexes was further supported by cyclic voltammetry through the presence of a catalytic current under CO_2 atmosphere. The D-π, π, and A-π complexes were studied to elucidate the effects of incorporating conjugated electron donating *vs.* withdrawing groups on the catalytic rates and product selectivity. The synthesized complexes were compared with $Re(bpy)(CO)_3Br$ (where bpy is 2,2′-bipyridine), the benchmark catalyst for this transformation. Remarkably, the complex with A-π pendant (**RC4**) outperformed the π (**RC2–3**) and D-π (**RC5**) complexes for the production of formic acid (HCO_2H) in the presence of photosensitizer $[Ru(bpy)_3]^{2+}$ and sacrificial electron donor BIH (1,3-dimethyl-2-phenyl-2,3-dihydro-1*H*-benzo[*d*]-imidazoline). Among the investigated catalysts, **RC4** with the A-π pendant showed the highest turnover number (TON) value of 844 for HCO_2H production with 86% carbon selectivity. In stark contrast to the imidazole-pyridine based catalysts reported here that favor formic acid as a product, $Re(bpy)(CO)_3Br$ generated no formic acid under the same conditions. The imidazole-pyridine complexes also function as catalysts for CO_2 reduction without an added photosensitizer, however, the TON values under self-sensitized conditions are poor.

Received 5th March 2025
Accepted 6th April 2025

DOI: 10.1039/d5ra01561h

rsc.li/rsc-advances

Introduction

Currently, CO_2 is the largest greenhouse gas emitted in the world.[1] There is a considerable effort to convert this relatively untapped waste product into renewable fuels. While the thermodynamic reduction potentials of transforming CO_2 to various products (CO, formic acid, methanol, methane, *etc.*) can be modest depending on the conditions,[2] the kinetics are slow and a catalyst is required to lower activation barriers and direct selectivity for the desired product.[3] Ideally, the energy required for catalysis is obtained directly from the sun or indirectly using solar photovoltaics to drive the electrochemistry. One reasonable goal for CO_2 valorization is to selectively reduce CO_2 to formic acid (HCO_2H), which can be used directly in formic acid fuel cells[4] or as a safe and easily transported H_2 storage material.[5,6] We note that CO is also a valuable product that can be transformed into hydrocarbon fuels *via* the Fischer–Tropsch process.[7]

The most well-studied mononuclear photocatalysts are derived from Lehn's original $Re(bpy)(CO)_3X$ (X = Cl, Br) catalyst,[8–10] which has been modified extensively with the goal to improve the catalytic performance.[11–14] Modification of the bidentate ligand has included introducing redox sites,[15] ancillary Lewis acids,[16] and other moieties to the second coordination sphere[17] (proton relays,[18] charged groups,[19] hydrogen bond donors[20,21]) to facilitate proton transfer events or stabilize intermediates,[8] change the local pH,[22] or increase the onset of visible light absorption.[23] Recently, Liang-Nian and coworkers reported an approach to increase the efficiency of the Re(bpy)-based photocatalyst by introducing chromophores onto the bipyridyl ligand, which yielded TONs as high as 1323 and Φ_{CO} up to 55%.[24] Another approach by Jurss and coworkers studied the effect of pendant light absorbing anthracene chromophores in mono- and di-nuclear anthracenyl Re(bpy) catalysts and found that especially in di-nuclear catalysts the ligand-based triplet state was highly influential.[25] With these two works as a conceptual backdrop, we seek to improve the overall light

[a]*Department of Chemistry, University of Kentucky, Lexington, KY 40506, USA. E-mail: aron.huckaba@uky.edu*

[b]*Department of Chemistry and Biochemistry, University of Mississippi, Mississippi 38677, USA*

† Electronic supplementary information (ESI) available. CCDC 2428908 and 2428909. For ESI and crystallographic data in CIF or other electronic format see DOI: https://doi.org/10.1039/d5ra01561h

‡ Co-first author.

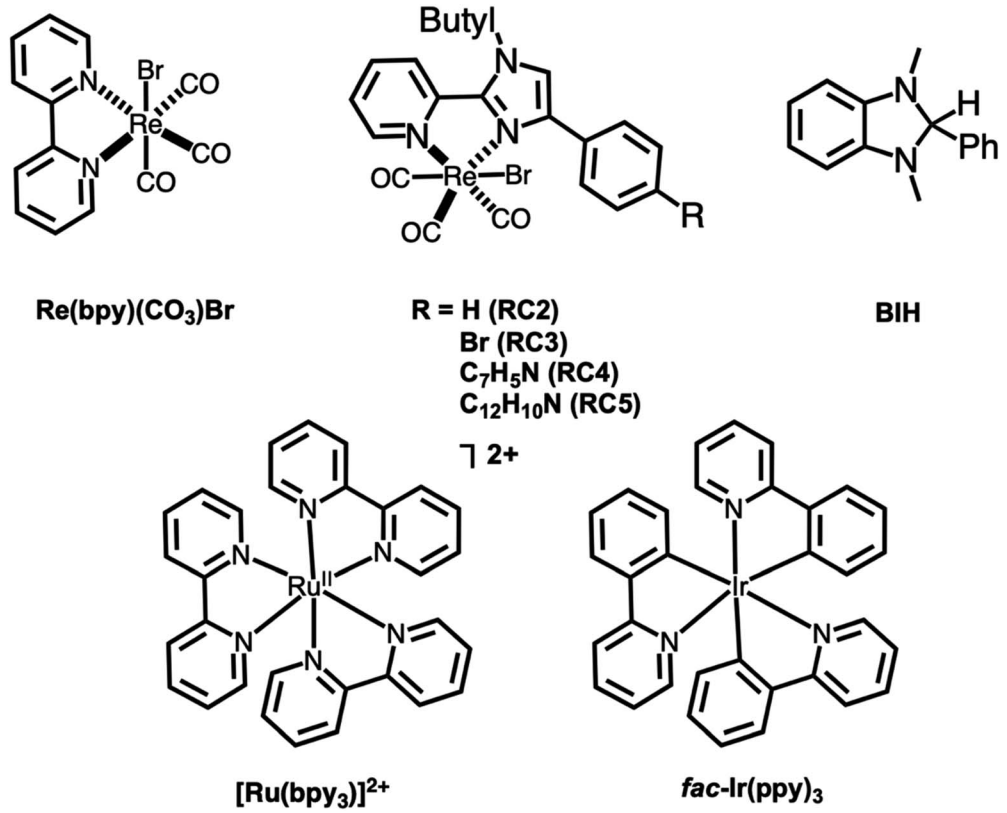

Fig. 1 Structures of complexes studied herein. The photosensitizers used and sacrificial electron donor (BIH) are also shown.

absorption and increase the activity for Re-based photocatalysts. We hypothesized that incorporating a ligand design with an enhanced charge transfer absorption, either in a donor–acceptor (D–A) or acceptor–donor (A–D) configuration would provide a strongly red-shifted charge transfer absorption.[26]

Herein, we report the synthesis, characterization, and catalytic activity of a series of novel Re(I) imidazolylpyridine complexes (Fig. 1). We were able to confirm two of the metal complex structures through single crystal X-ray diffraction. The electrocatalytic and photocatalytic trials indicated that the complexes are able to reduce CO_2 in sensitized photocatalytic reactions, and were modestly selective for HCO_2H, which is rare for this class of Re photocatalysts.[27–29]

Results and discussion

Catalyst synthesis

The synthesis of complexes **RC2** and **RC3** begin with an imidazole forming condensation between the alpha-brominated ketones **2**, **5**, or **10** and 2-amidinylpyridine to afford **3**, **6**, and **11** (Scheme 1).[30] Imidazole alkylation with 1-bromobutane using NaH afforded **4**, **7**, and **12** in moderate yields. Alkylation of the imidazole unit was crucial to the success of the synthesis as the non-alkylated pyridyl-imidazole ligand was observed to chelate the Re metal center using either of the imidazole N atoms due to tautomerization. This led to mixtures of the two possible isomers that were not separable.[31] Upon alkylation, however, only one isomer was observed to form, and Nuclear Overhauser Effect (NOESY) spectroscopy was performed to confirm which isomer was present after purification (Fig. S4†). Refluxing $Re(CO)_5Br$ in toluene with **4**, **7**, or **12** afforded catalysts **RC2**, **RC3**, or **RC4**. Catalyst **RC5** was afforded with relative ease by Buchwald-coupling of diphenylamine with **7**, followed by metalation with $Re(CO)_5Br$ in refluxing toluene. Suzuki-coupling of 3-cyanophenylboronic acid and 4-bromoacetophenone was performed to afford **9** which was then brominated at the ketone α carbon with NBS and *p*-toluenesulfonic acid to give **10**. Detailed procedures for the synthesis of the ligands and their corresponding Re complexes is described in the ESI.†

Crystallographic data

Suitable single crystals of **RC2** and **RC3** were obtained *via* vial-in-vial vapor diffusion using methylene chloride in the inner vial and diethyl ether in the outer vial after allowing the set-up to stand overnight (Fig. 2). Both crystals were bright yellow in color. Other instances of diimine pyridyl-imidazole rhenium crystals have been reported in the literature and a comparison of the selected bond lengths with a reference complex can be found below. The crystallographic data are summarized in Table 1. The Re1–$N_{imidazole}$ and Re1–$N_{pyridine}$ bond lengths are slightly shorter (0.005 Angstroms) in **RC2** than **RC3**, likely owing to the electron withdrawing nature of the bromine substituent lengthening the Re–N bonds in **RC3**. The $N_{imidazole}$–Re bond length in **RC2** (2.181(2) Å) is longer than an analogous bond

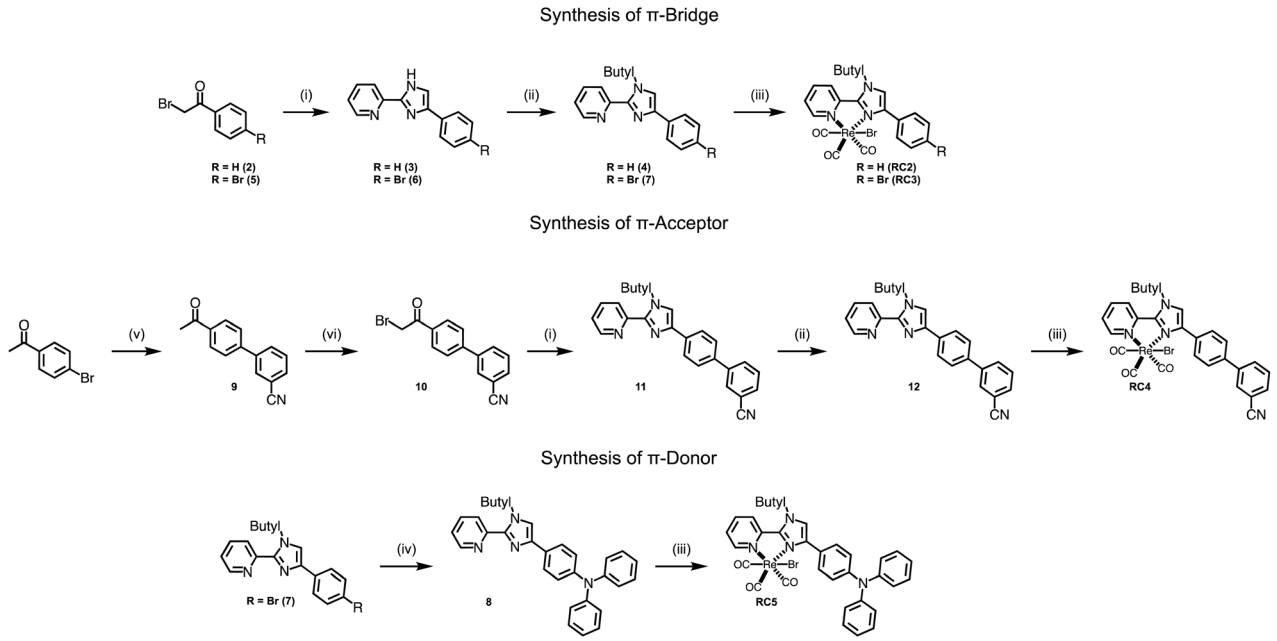

Scheme 1 Synthetic steps to prepare complexes **RC2–RC5**. Reaction conditions: (i) $KHCO_3$, H_2O, THF, amino(pyridin-2-yl)methaniminium chloride, reflux. Yields: **3**: 70%; **6**: 70%; **11**: 75%. (ii) 1-Bromobutane, DMF, NaH, 80 °C. Yields: **4**: 60%; **7**: 77%; **12**: 30%. (iii) $Re(CO)_5Br$, toluene, reflux. Yields: **13**: 55%; **14**: 57%; **15**: 23%; **16**: 60%. (iv) Diphenyl amine, toluene, KO*t*Bu, $Pd(dba)_2$, tri-*tert*-butylphosphonium tetrafluoroborate, reflux, 76%. (v) 3-Cyanophenylboronic acid, Na_2CO_3, $Pd(PPh_3)_4$, 5 : 1 dioxane : water, 72%. (vi) *p*-TsOH, NBS, MeCN, reflux, 60%.

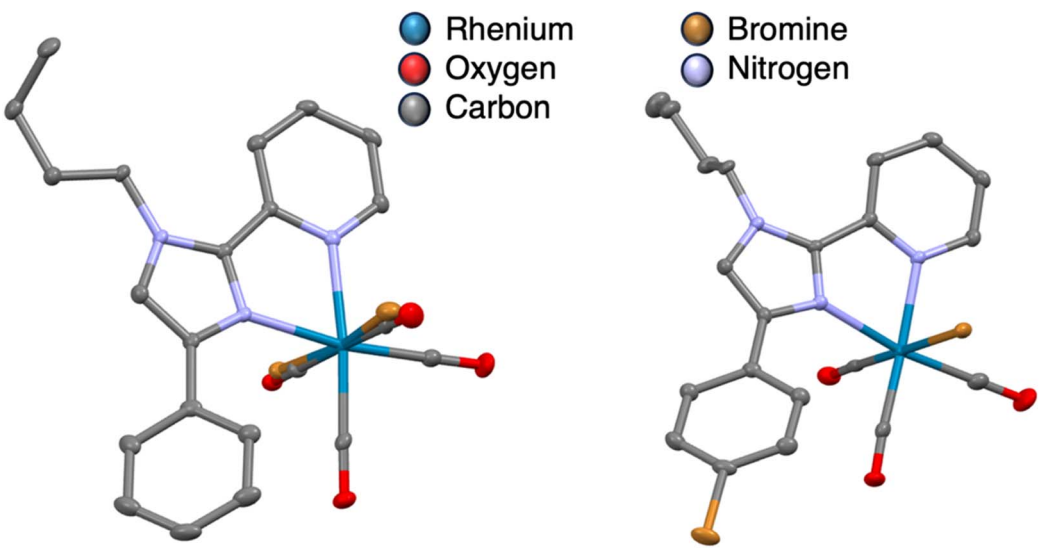

Fig. 2 Crystal structures of **RC2** (left) **RC3** (right) omitting hydrogen atoms for clarity.

found in a benzimidazolylpyridine Re(I) complex (2.130(1) Å), indicating a weaker N–Re bond for the imidazole donor of **RC2**.[32,33] Similarly, in a Re–pyridylimidazole complex with a 4-(*N*,*N*-dimethylamino)pyridine group instead of a bromine substituent, the $N_{imidazole}$–Re bond length is shorter as well (2.118 Å). This indicates that in **RC2**/**RC3**, the bond lengths are longer than those observed for related Re(azolylpyridine) complexes.

UV-Vis analysis

To characterize the light absorption properties of each complex, UV-visible absorption spectra were collected of the complexes dissolved in acetonitrile (MeCN) and are shown in Fig. 3. The optical properties of the complexes are summarized in Table 2. The data from these experiments revealed that the absorption onsets (λ_{onset}) of **RC2–4** are blue-shifted compared to **1**, in contrast to our hypothesis. We reason the blue shifts are due to the increased basicity of the imidazole donor in comparison to

Table 1 Crystallographic data of catalysts RC2 and RC3

	RC2	RC3
Empirical formula	$C_{21}H_{19}BrN_3O_3Re$	$C_{21}H_{18}Br_2N_3O_3Re$
Formula weight	627.50	706.40
Crystal system	Orthorhombic	Monoclinic
Space group (no.)	*Pbca*	$P2_1/c$
a (Å)	14.4135 (6)	11.7322 (3)
b (Å)	13.9657 (5)	11.2485 (2)
c (Å)	19.9434 (9)	17.8809 (4)
α (deg)	90	90
β (deg)	90	104.108
γ (deg)	90	90
V (Å^3)	4014.5 (3)	2288.56
Z	8	4
F(000) (e)	2400	1336
μ (Mo-Kα) (mm^{-1})	8.073	
Reflections collected	43 216	46 047
Independent reflections	4593 (R_{int} = 0.0474)	5254 (R_{int} = 0.0310)
Observed reflections ($F_o \geq 2\sigma(F_o)$)	43 216	46 047
Refined parameters	280	273
Goodness-of-fit on F^2	1.163	1.057
R_a, R_{wb} ($I \geq 2\sigma(I)$)	0.0195, 0.0434	0.0149, 0.0292
R_a, R_{wb} (all data)	0.0212, 0.0440	0.0179, 0.0299

pyridine, in addition to the lower degree of conjugation in the imidazole ring. Complex **RC5** shares a similar λ_{onset} to **1** at 425 nm. From the compounds, **RC5** possesses the largest molar absorptivity coefficient while also possessing the most red-shifted MLCT absorption band in the visible light region. Interestingly, complexes **RC2** and **RC3** differ considerably in their molar absorptivity ($\Delta\varepsilon$ = 5853 M^{-1} cm^{-1}) with the substitution of just one hydrogen for a bromine atom.

Electrochemical analysis

The redox properties of **RC2–5** were measured using cyclic voltammetry (CV) to examine whether the complexes could serve as CO_2 reduction catalysts under a CO_2 atmosphere and shown in Fig. 4 and summarized in Table 3. When CO_2 was sparged into each solution of dissolved complex, there was an increase in current associated with the first reduction potential, indicative

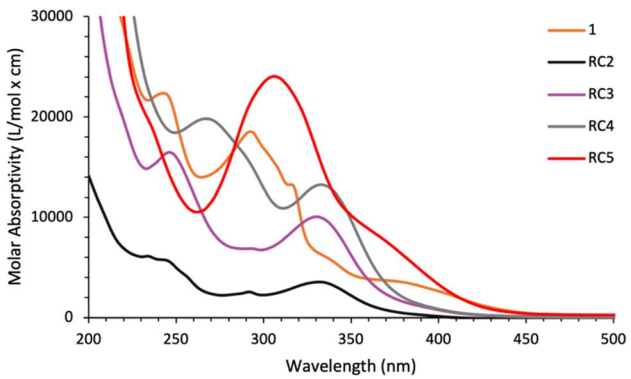

Fig. 3 UV-Vis absorption spectra for catalysts **1**–**RC5** dissolved in MeCN.

Table 2 Optical properties of catalysts **1** and **RC2–5**[a]

Catalyst	λ_{max} (nm)	λ_{onset}[c] (nm)	ε (M^{-1} cm^{-1})	$E_{MLCT\text{-}GS}$[d] (eV)
1	292, 384[b]	420	18 951	2.95
RC2	248, 337[b]	370	3718	3.35
RC3	246, 331[b]	375	9571	3.31
RC4	267, 336[b]	380	19 855	3.26
RC5	306, 371[b]	425	23 381	2.92

[a] Measured in acetonitrile. [b] Indicates shoulder. [c] Estimated from the intercept of the baseline and a tangent line on the UV-Vis spectrum on the low energy side of the absorption. [d] Estimated from the onset of the low energy side of the absorption curve. The $E_{MLCT\text{-}GS}$ was converted from nm to eV using the equation $1240/E_{MLCT\text{-}GS}$ nm = $E_{MLCT\text{-}GS}$ eV.

of catalytic CO_2 reduction activity. The increase in current for complexes **RC2** and **RC3** was also accompanied by shifts in the reduction wave to higher energy, while the current for **RC5** was accompanied by a shift in the reduction wave to a lower energy.

These measurements are also useful for determining whether the excited state reduction potentials of each complex are appropriately positioned for electron transfer from sacrificial electron donors like BIH or from photosensitizers (PS) such as Ir(ppy)$_3$ or [Ru(bpy$_3$)]$^{2+}$. An energy level diagram showing relevant reduction potentials associated with the rhenium catalysts, the aforementioned photosensitizers, the standard reduction potential of CO_2 to CO, and sacrificial electron donors BIH and TEA is given in Fig. 5. The reduction potentials of the dissolved complexes in nitrogen-sparged MeCN fall between −1.30 and −1.55 V *vs.* saturated calomel electrode (SCE), all of which are relatively higher in energy than the reduction potential of Re(bpy)(CO)$_3$Br. The reduction potentials are also lower or very nearly lower in energy than both Ir(ppy)$_3$ or [Ru(bpy$_3$)]$^{2+}$, which suggests that either could serve as a PS for the complexes. The excited state reduction potential of each complex falls between 1.59 and 2.01 V *vs.* SCE, which are all substantially lower than the oxidation potentials of both BIH and triethanolamine (TEOA) or triethylamine (TEA), which indicates that each can serve as an electron donor.

Photocatalytic CO_2 reduction

The Re complexes were applied to the photocatalytic reduction of CO_2 using anhydrous MeCN as the reaction solvent and a natural white light LED light source (λ > 400 nm) adjusted to 1 Sun intensity. Following initial optimization experiments (Table S2†) with catalyst **RC2** and **RC5**, [Ru(bpy)$_3$]$^{2+}$ was selected as a PS due to its superior performance for photocatalytic CO_2 reduction compared to Ir(ppy)$_3$. A sacrificial electron donor BIH was used with TEOA where TEOA plays a secondary role as a base in deprotonating the BIH radical cation generated in the initial electron transfer process to the excited PS to limit back electron transfer.[39] TEOA was chosen as the amine to pair with BIH as it gave better activity compared to another commonly used base, TEA. TEOA has been shown to react with CO_2 to form a zwitterionic alkylcarbonate adduct that serves to capture CO_2 in solution and facilitate proton transfer events.[40] Gaseous products such as carbon monoxide (CO), methane (CH_4), and

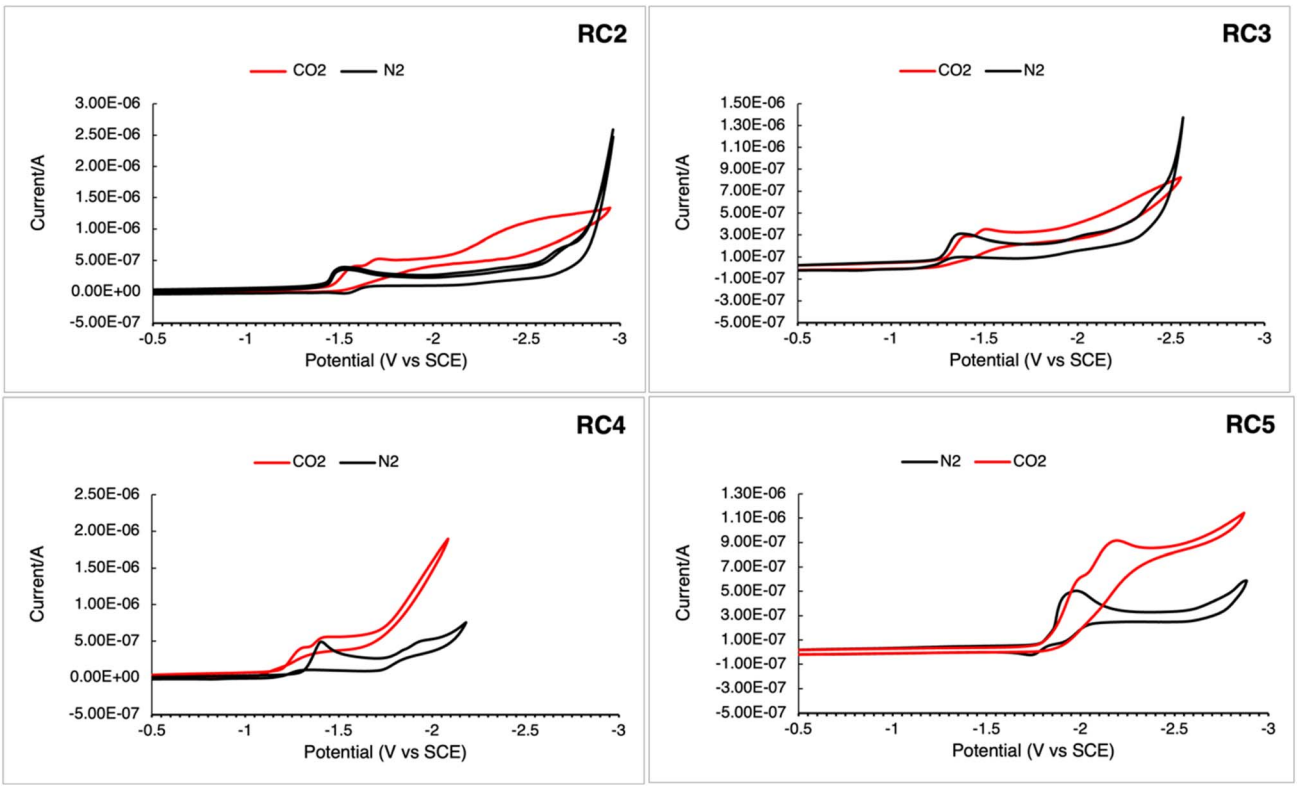

Fig. 4 Cyclic voltammograms of catalysts **RC2–RC5**. Spectra were recorded in dry MeCN, 0.1 M Bu_4NPF_6 in MeCN using a Pt pseudo-reference, Pt counter, and glassy carbon working electrode using a scan rate of 0.1 V s^{-1}. All spectra were referenced to ferrocene (Fc) as an internal standard using the Fc^+/Fc = 0.4 V couple *vs.* SCE.[38]

Table 3 Electrochemical properties of catalysts **RC2–RC5**[a]

Catalyst	$E_{(S+/S)}$[b] (V)	$E_{(S-/S)}$[c] (V)	$E_{(S*/S-)}$[d] (V)
1 (ref. 11)	1.26	−1.20	1.33
RC2	1.40	−1.35	2.00
RC3	1.45	−1.30	2.01
RC4	1.40	−1.35	1.91
RC5	0.85	−1.55	1.59
$[Ru(bpy_3)]^{2+}$ (ref. 34)	1.29	−1.33	0.31
fac-$Ir(ppy)_3$ (ref. 34)	0.73	−2.19	0.34

[a] Measured in dry MeCN. All values are reported *vs.* SCE and were measured by CV in 0.1 M Bu_4NPF_6 in MeCN using a Pt pseudo-reference, Pt counter, and a glassy carbon working electrode. [b] Estimated as the onset of the oxidation peak due to irreversibility of the wave. [c] Estimated as the onset of the reduction peak due to irreversibility of the wave. [d] Estimated *via* the sum of the reduction potential and $E_{MLCT\text{-}GS}$ using the equation: $E_{(S*/S-)} = E_{(S-/S)} + E_{MLCT\text{-}GS}$.

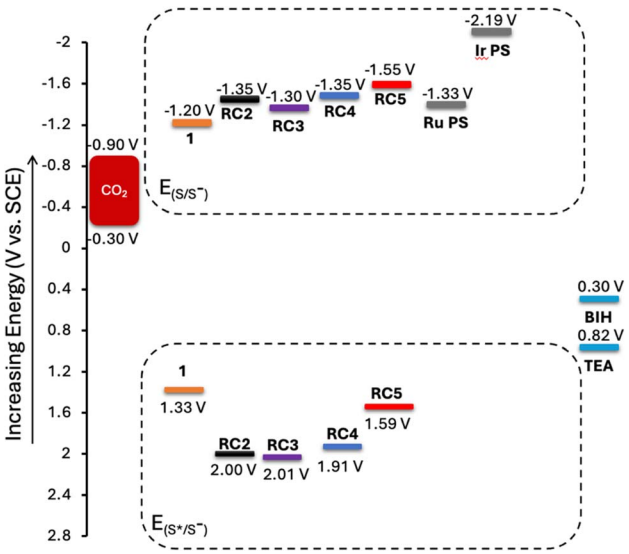

Fig. 5 Energy level diagram illustrating of catalyst reduction potentials, calculated excited-state reduction potentials from the $E_{MLCT\text{-}GS}$ values, approximated range for the standard $2e^-/2H^+$ reduction potential of CO_2 to CO (and H_2O) in acetonitrile based on the minimum and maximum pH range in the photocatalytic trials, and the oxidation potentials of BIH and TEA.[35–37]

hydrogen (H_2) were detected and quantified by gas chromatography (GC). Formic acid (HCO_2H) as a solution-phase product of the photocatalytic reactions was quantified by ^1H NMR spectroscopy using ferrocene as an internal standard. The detailed procedure for quantifying HCO_2H and a representative ^1H NMR spectrum for this measurement is given in the ESI (Fig. S7†).

The results of photocatalytic CO_2 reduction experiments are summarized and shown in Table 4 and Fig. 6. In the presence of PS $[Ru(bpy)_3]^{2+}$ and electron donor BIH, Re-complexes **RC2–5** were found to be active in light-driven CO_2 reduction with observed products HCO_2H, CO, and H_2. At a catalyst

Table 4 Performance comparison of the catalysts in the photocatalytic reduction of CO_2[a]

Entry	Catalyst	HCO_2H (TON[b])	CO (TON[b])	H_2 (TON[b])	CS[c] (%)
1	**RC4**	844	88	148	86
2	**RC3**	593	126	362	67
3	**RC2**	280	150	224	66
4	**RC5**	275	113	266	59
5	**1**[d]	0	436	222	67

[a] Reactions were conducted in anhydrous MeCN with 1 μM catalyst/2 mL, 0.1 mM $[Ru(bpy)_3]^{2+}$, 50 mM BIH, and 5% (v/v) TEOA/MeCN. [b] Turnover number (TON) values are reported at 72 h after catalysis was no longer occurring. [c] Carbon-selective (CS) reduction percentage is calculated as CS% = [(CO TON + CH_4 TON + HCO_2H TON)/total observed product TON × 100]. [d] Previously published; no HCO_2H formation.

concentration of 1 μM, CO_2 is primarily reduced to HCO_2H as the dominant product, accompanied by H_2 as a secondary byproduct from proton reduction. A smaller amount of CO was also formed. Interestingly, catalyst **RC4**, having resonance π-A group, exhibited the best catalytic performance for CO_2 reduction with a turnover number (TON) value of 844 for HCO_2H production and the highest selectivity for CO_2 reduction products of 86% (Table 4, entry 1 and Fig. 6 (right)). Catalysts **RC2** (TON for HCO_2H = 280) and **RC5** (TON for HCO_2H = 275) with π-bridge and π-D group, respectively, showed lower catalytic activity overall than **RC4**, but similar activities and selectivities to one another with **RC2** having a modestly higher carbon selectivity percentage (Table 4 and Fig. 6). Complex **RC3** with Br-substituted π-bridge gave the second highest TON value for HCO_2H of 593, which exceeds **RC5** and the structurally similar complex **RC2**, but also produced the largest TON value for H_2 at 362. This photocatalytic study establishes a clear correlation between the electron withdrawing π-A (–PhCN) and electron donating π-D ($-NPh_2$) substituents attached to the imidazole ring. Among the catalysts investigated, the best performance was observed from the Re complex **RC4** which contains a π-A group, followed by less electron withdrawing Br-substituted π-bridge **RC3**. Electronically neutral catalyst **RC2** and π-D group substituted **RC5** showed the lowest TON value for HCO_2H generation. Notably, no HCO_2H was observed for benchmark catalyst **1**. A recent publication described that $[Re(bpy)_2(CO)_2]^+$ also selectively formed HCO_2H with a TON value of 428 from CO_2 reduction, and they proposed a catalytic cycle similar to that of ruthenium catalyst $[Ru(bpy)_2(CO)_2]^{2+}$.[28] Doyle and coworkers have reported a photocatalyst, $Re(CO)_3$(1-(1,10) phenanthroline-5-(4-nitro-naphthalimide))Cl, which is selective for HCO_2H generation with a TON value of 533.[41] We propose that the catalysts reported here also utilize the same catalytic cycle as that reported by Richeson and coworkers, which features a Re–H intermediate that undergoes CO_2 insertion to give a Re–formato intermediate.[28] Each of the imidazole-pyridine based catalysts reported here generate a mixture of HCO_2H, CO, and H_2 with HCO_2H being the dominant product overall; likewise, TON values for H_2 are greater than those of CO. The highest TON values for HCO_2H production were obtained with catalysts bearing electron withdrawing substituents (**RC3** and **RC4**) on the imidazole donor with HCO_2H : H_2 ratios of 5.7 (**RC4**) and 1.6 (**RC3**). The catalysts with more electron donating substituents (**RC2** and **RC5**) slightly favor HCO_2H, but with lower TON values and HCO_2H : H_2 ratios closer to 1. A rhenium-hydride species[28] is expected to be a common intermediate responsible for the production of HCO_2H and H_2 during catalysis, both of which are formed in higher quantities than CO. The competition between HCO_2H and H_2 suggests that the hydricity of the putative Re–H is near 44 kcal mol^{-1} (*i.e.* the hydricity of formate in acetonitrile)[42] and sensitive to the ligand substitutions. To the best of our knowledge, Re complex **RC4** sets a new benchmark with the highest TON value for HCO_2H production of 844 reported for rhenium-based CO_2 reduction catalysts.

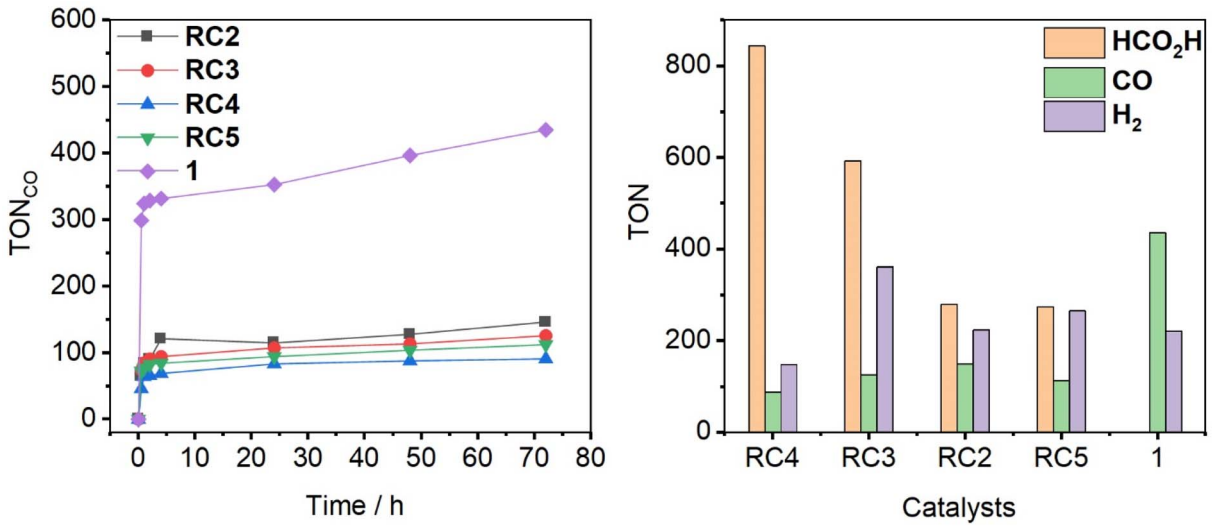

Fig. 6 CO formation over 72 h period (left) and the production of HCO_2H, CO, and H_2 after 72 h (right) in photocatalytic CO_2 reduction reaction with catalysts **RC2**, **RC3**, **RC4**, **RC5**, and **1**. All experiments were performed with 1 μM catalyst, 50 mM BIH, 0.1 mM $[Ru(bpy)_3]^{2+}$, and 5% (v/v) TEOA in anhydrous MeCN solution. The data points given are the average of two sample runs.

Under the same conditions, complex **1** outperformed catalyst **RC2–5** regarding CO production (Fig. 6 and Table 4, entry 5). Comparing catalysts **RC2–5**, catalyst **RC2** with a π-bridge on the imidazole ring showed comparatively better catalytic activity with a TON value of 150 for CO generation. In contrast, **RC4** exhibited a relatively low TON value of 88 for CO evolution, strongly favoring HCO_2H production. Toward H_2 production, the highest activity ($TON_{H_2} = 362$) was observed for complex **RC3**, followed by **RC2** and **RC5**, with complex **RC4** giving the lowest TON value for H_2 (Table 4).

Catalytic performance of **RC2–5** was also evaluated without using an external PS (Table S1†). Although the parent complex **1** is known to exhibit self-sensitized catalytic activity ($TON_{CO} = 55$), only one of the Re complexes (**RC5**) absorbed visible light. Each of the catalysts exhibited very poor self-sensitized photocatalytic activity. Therefore, we conclude that catalysts **RC2–RC5** required a PS for significant catalysis to occur.

The influence of catalyst concentration on TON values was also investigated using complexes **RC4** and **RC2** (Table 5). The TON values decreased dramatically when the catalyst concentration was changed from 1 μm to 10 and 100 μM. This is a typical result, as lowering the catalyst concentration has been shown to result in higher TON values owing to the catalytic sites being isolated from one another, therefore reducing deleterious side reactions.[43,44]

The control experiments were performed using complex **RC2** to determine the necessity of each component used in the photocatalytic CO_2 reduction. The outcomes of these experiments are summarized in Table 6, where entry 1 is the result of our standard condition (all components present). Photocatalysis under N_2 in the absence of CO_2, or without the rhenium catalyst, or without irradiation (entries 5–7), resulted in negligible product formation, indicating the necessity of the substrate, the Re catalyst, and light, respectively. The impact of removing the PS (TON_{HCO_2H} with PS = 280 and without PS = 0, entries 1 and 2) and removing the electron donor BIH (TON_{HCO_2H} with BIH = 280 and without BIH = 10, entries 1 and 3) is significant. BIH is a better electron donor (more driving force for electron transfer) than TEOA, and thus, better catalytic activity is observed in the presence of BIH compared to using TEOA alone as the sacrificial electron donor. Interestingly, in the absence of TEOA, catalyst **RC2** showed similar TON values for HCO_2H compared to the experiment with TEOA (Table 6, entries 1 and 4). However, lower TON values for CO and higher values for H_2 production are also observed without TEOA, indicating that the presence of TEOA strongly influences product selectivity.

Table 5 Results of photocatalytic CO_2 reduction with RC2 and RC4 at different catalyst concentrations[a]

[Catalyst] (μM)	Catalyst	HCO_2H (TON)	CO (TON)	H_2 (TON)	CS[b] (%)
1	**RC4**	844	88	148	86
	RC2	280	150	224	66
10	**RC4**	53	16	18	79
	RC2	20	69	29	75
100	**RC4**	17	8	3	89
	RC2	8	6	5	74

[a] Maintained a constant irradiation time of 72 h and the same reaction conditions provided in Table 1. [b] CS% = [(CO TON + CH_4 TON + HCO_2H TON)/total observed product TON × 100].

Table 6 Summary of the photocatalytic control experiments with catalyst RC2[a]

Entry	Catalyst	PS[b]	e^- donor[c]	CO (TON)	H_2 (TON)	HCO_2H (TON)
1	2	Yes	BIH, TEOA	150	224	280
2	2	No	BIH, TEOA	2	9	0
3	2	Yes	TEOA	16	14	10
4	2	Yes	BIH	45	388	228
5[d]	2	Yes	BIH, TEOA	2	1	0
6	None	Yes	BIH, TEOA	1	1	0
7[e]	2	Yes	BIH, TEOA	0	0	0

[a] Irradiation time was constant at 72 h. The activity under standard conditions is provided in entry 1. [b] PS = $[Ru(bpy)_3]^{2+}$. [c] When both components are listed both are present. [d] Under nitrogen atmosphere. [e] No irradiation.

In Table 7, catalysts **RC2–5** are compared to recent Re(I) catalysts applied to light-driven CO_2 reduction in the presence of a sacrificial electron donor. Müller *et al.*[45] recently synthesized three rhenium tricarbonyl catalysts that produce TON values for CO as high as 125 without the presence of an external PS and using TEOA as the sacrificial electron donor. These excellent TON_{CO} values were achieved by relatively simple modification to a 1,10-phenanthroline core by adding different heterocyclic substitutions at the 4 and 7 positions. Rotundo *et al.*[46] also achieved similar TON_{CO} values of 120 with $Re^I(CO)_3$ catalysts using BIH instead of TEOA while studying the effects of substituted 2,2′-bipyridine based ligands containing various functional groups in the second-coordination sphere. Liang and coworkers[24] reported a self-sensitized rhenium catalyst utilizing pendant dipyrromethene-BF_2 chromophores linked to a 2,2′-bipyridine core to achieve TON_{CO} values as high as 1376 with BIH as the sacrificial electron donor. Although catalyst **RC2** possesses similar TON_{CO} values to Müller's and Rotundo's catalysts, their compounds function as effective self-sensitized photocatalysts while **RC2** does not. With respect to formic acid production, **RC4** in particular performs remarkably well compared to most Re catalysts that are generally known for their high selectivity for CO_2-to-CO conversion. However, there are two recent rhenium catalysts that preferentially produce HCO_2H. Spear *et al.*[27] recently synthesized a rhenium catalyst supported by a phenanthroline nitro-naphthalimide ligand which selectively produced HCO_2H in the absence of an external PS with a TON value as high as 533. Hameed *et al.*[28] also achieve high selectivity and a HCO_2H TON value of 428 utilizing the triflate salt of a bis(-bipyridine) dicarbonyl rhenium complex which becomes less selective for HCO_2H over the course of the reaction. Catalyst **RC4** in comparison yields greater TON values for HCO_2H, but

Table 7 Summary of the catalytic performance of selected rhenium catalysts applied to light-driven CO_2 reduction

Catalyst	PS	e^- donor	CO (TON)	H_2 (TON)	HCO_2H (TON)	CS[d] (%)
RC4	$[Ru(bpy)_3]^{2+}$	BIH, TEOA	88	148	844	86
RC4	No	BIH, TEOA	5	1	0	85
fac-[Re(NN)[a](CO)$_3$Cl][45]	No	TEOA	125	nd	nd	100
fac-[ReCl(L)[b](CO)$_3$][46]	No	BIH	120	nd	nd	100
[Re(BDP)$_2$[c]][24]	$[Ru(bpy)_3]^{2+}$	BIH	1376	nd	nd	100
[Re(CO)$_3$(1-(NN)[a]-5-(4-nitro-napthalimide))Cl][27]	No	BIH	0.04	nd	533	100
cis-[Re(bpy)$_2$(CO$_2$)]$^+$OTf$^-$(1$^+$OTf$^-$)[28]	$[Ru(bpy)_3]^{2+}$	BIH, TEOA	nd	38	428	92

[a] NN = 1,10-phenanthroline having pyrrole. [b] L = Ph-NH_2 substituted 2,2′-bipyridine. [c] BDP = 2,2′-bipyridine having dipyrromethene-BF_2 chromophores. [d] CS% = [(CO TON + HCO_2H TON)/total observed product TON × 100].

with lower selectivity due to the formation of CO and H_2, products that are not generated in large quantities or at all with the other two catalysts.

Conclusions

Carbon dioxide valorization to fuels or fuel precursors is an attractive strategy to reduce the overall use of non-renewable carbon fuel sources. Here, we synthesized four novel imidazolyl-pyridine Re complexes that were applied to the photocatalytic reduction of CO_2 and compared to benchmark catalyst Re(bpy)(CO)$_3$Br, **1**. By replacing one of the pyridyl rings for a substituted imidazole group containing electron donating or accepting moieties, we were able to tune the electronic properties and light absorption of the complexes. Of note is that each of the imidazolyl complexes favored HCO_2H production, which is unusual for Re(CO)$_3$ based catalysts which overwhelming mediate the conversion of CO_2-to-CO with high selectivity. Catalysts **RC3** and **RC4** strongly favored HCO_2H generation, with **RC4** being the most active and selective catalyst overall with an overall carbon selectivity (CS) of 86%. The CS percentage of **RC3** is 67% due to a relatively large TON value for H_2 evolution. Catalysts **RC2** and **RC5** also favor HCO_2H as the dominant CO_2 reduction product but make comparably higher amounts of CO and H_2 and thus have lower carbon selectivity of 66 and 59%, respectively. In sharp contrast, benchmark catalyst **1** does not produce HCO_2H under the same conditions. The production of HCO_2H is rare for rhenium-based catalysts for CO_2 reduction with only a few examples known in the literature. Catalyst **RC4** gave a TON value for HCO_2H as high as 844 at 1 μM catalyst concentration, further demonstrating the high stability of this catalyst under photochemical conditions.

Data availability

The data supporting this article have been included as part of the ESI.† CCDC 2428908 and 2428909 contain the supplementary crystallographic data for this paper. These data can be obtained free of charge *via* **http://www.ccdc.cam.ac.uk/data_request/cif**, or by emailing data_request@ccdc.cam.ac.uk, or by contacting The Cambridge Crystallographic Data Centre, 12 Union Road, Cambridge CB2 1EZ, UK; fax: +44 1223 336033.

Conflicts of interest

There are no conflicts to declare.

Acknowledgements

M. I. S. and J. W. J. thank the National Science Foundation for generous funding through a CAREER award (CHE-1848478).

References

1 U. S. E. P. Agency, Overview of Greenhouse Gases, **https://www.epa.gov/ghgemissions/overview-greenhouse-gases**.
2 E. E. Benson, C. P. Kubiak, A. J. Sathrum and J. M. Smieja, Electrocatalytic and homogeneous approaches to conversion of CO_2 to liquid fuels, *Chem. Soc. Rev.*, 2009, **38**(1), 89–99.
3 X. Zhang, S.-X. Guo, K. A. Gandionco, A. M. Bond and J. Zhang, Electrocatalytic carbon dioxide reduction: from fundamental principles to catalyst design, *Mater. Today Adv.*, 2020, **7**, 100074.
4 Z. Ma, U. Legrand, E. Pahija, J. R. Tavares and D. C. Boffito, From CO_2 to Formic Acid Fuel Cells, *Ind. Eng. Chem. Res.*, 2021, **60**(2), 803–815.
5 F. Joó, Breakthroughs in Hydrogen Storage—Formic Acid as a Sustainable Storage Material for Hydrogen, *ChemSusChem*, 2008, **1**(10), 805–808.
6 J. Eppinger and K.-W. Huang, Formic Acid as a Hydrogen Energy Carrier, *ACS Energy Lett.*, 2017, **2**(1), 188–195.
7 H. Jahangiri, J. Bennett, P. Mahjoubi, K. Wilson and S. Gu, A review of advanced catalyst development for Fischer–Tropsch synthesis of hydrocarbons from biomass derived syn-gas, *Catal. Sci. Technol.*, 2014, **4**(8), 2210–2229.
8 J. Hawecker, J.-M. Lehn and R. Ziessel, Efficient photochemical reduction of CO_2 to CO by visible light irradiation of systems containing Re(bipy)(CO)$_3$X or $Ru(bipy)_3^{2+}$–Co^{2+} combinations as homogeneous catalysts, *J. Chem. Soc. Chem. Commun.*, 1983, (9), 536–538.
9 J. Hawecker, J.-M. Lehn and R. Ziessel, Electrocatalytic reduction of carbon dioxide mediated by Re(bipy)(CO)$_3$Cl (bipy = 2,2′-bipyridine), *J. Chem. Soc. Chem. Commun.*, 1984, (6), 328–330.

10 J. Hawecker, J.-M. Lehn and R. Ziessel, Photochemical and Electrochemical Reduction of Carbon Dioxide to Carbon Monoxide Mediated by (2,2′-Bipyridine) tricarbonylchlororhenium(I) and Related Complexes as Homogeneous Catalysts, *Helv. Chim. Acta*, 1986, **69**(8), 1990–2012.

11 L. Kearney, M. P. Brandon, A. Coleman, A. M. Chippindale, F. Hartl, R. Lalrempuia, M. Pižl and M. T. Pryce, Ligand-Structure Effects on *N*-Heterocyclic Carbene Rhenium Photo- and Electrocatalysts of CO_2 Reduction, *Molecules*, 2023, **28**(10), 4149.

12 S. Sinha, E. K. Berdichevsky and J. J. Warren, Electrocatalytic CO_2 reduction using rhenium(I) complexes with modified 2-(2′-pyridyl)imidazole ligands, *Inorg. Chim. Acta*, 2017, **460**, 63–68.

13 H. Y. V. Ching, X. Wang, M. He, N. Perujo Holland, R. Guillot, C. Slim, S. Griveau, H. C. Bertrand, C. Policar, F. Bedioui and M. Fontecave, Rhenium Complexes Based on 2-Pyridyl-1,2,3-triazole Ligands: A New Class of CO_2 Reduction Catalysts, *Inorg. Chem.*, 2017, **56**(5), 2966–2976.

14 L. Rotundo, E. Azzi, A. Deagostino, C. Garino, L. Nencini, E. Priola, P. Quagliotto, R. Rocca, R. Gobetto and C. Nervi, Electronic Effects of Substituents on *fac*-M(bpy-R)$(CO)_3$ (M = Mn, Re) Complexes for Homogeneous CO_2 Electroreduction, *Front. Chem.*, 2019, **7**, 417.

15 R. Stichauer, A. Helmers, J. Bremer, M. Rohdenburg, A. Wark, E. Lork and M. Vogt, Rhenium(I) Triscarbonyl Complexes with Redox-Active Amino- and Iminopyridine Ligands: Metal–Ligand Cooperation as Trigger for the Reversible Binding of CO_2 via a Dearmomatization/Rearomatization Reaction Sequence, *Organometallics*, 2017, **36**(4), 839–848.

16 A. J. M. Miller, J. A. Labinger and J. E. Bercaw, Homogeneous CO Hydrogenation: Ligand Effects on the Lewis Acid-Assisted Reductive Coupling of Carbon Monoxide, *Organometallics*, 2010, **29**(20), 4499–4516.

17 S. S. Roy, K. Talukdar and J. W. Jurss, Electro- and Photochemical Reduction of CO_2 by Molecular Manganese Catalysts: Exploring the Positional Effect of Second-Sphere Hydrogen-Bond Donors, *ChemSusChem*, 2021, **14**(2), 662–670.

18 A. Wilting, T. Stolper, R. A. Mata and I. Siewert, Dinuclear Rhenium Complex with a Proton Responsive Ligand as a Redox Catalyst for the Electrochemical CO_2 Reduction, *Inorg. Chem.*, 2017, **56**(7), 4176–4185.

19 S. Sahu, P. L. Cheung, C. W. Machan, S. A. Chabolla, C. P. Kubiak and N. C. Gianneschi, Charged Macromolecular Rhenium Bipyridine Catalysts with Tunable CO_2 Reduction Potentials, *Chem.–Eur. J.*, 2017, **23**(36), 8619–8622.

20 J. O. Taylor, G. Neri, L. Banerji, A. J. Cowan and F. Hartl, Strong Impact of Intramolecular Hydrogen Bonding on the Cathodic Path of [Re(3,3′-dihydroxy-2,2′-bipyridine)$(CO)_3$Cl] and Catalytic Reduction of Carbon Dioxide, *Inorg. Chem.*, 2020, **59**(8), 5564–5578.

21 A. N. Hellman, R. Haiges and S. C. Marinescu, Rhenium bipyridine catalysts with hydrogen bonding pendant amines for CO_2 reduction, *Dalton Trans.*, 2019, **48**(38), 14251–14255.

22 L. Rotundo, C. Garino, E. Priola, D. Sassone, H. Rao, B. Ma, M. Robert, J. Fiedler, R. Gobetto and C. Nervi, Electrochemical and Photochemical Reduction of CO_2 Catalyzed by Re(I) Complexes Carrying Local Proton Sources, *Organometallics*, 2019, **38**(6), 1351–1360.

23 L.-Q. Qiu, K.-H. Chen, Z.-W. Yang and L.-N. He, A rhenium catalyst with bifunctional pyrene groups boosts natural light-driven CO_2 reduction, *Green Chem.*, 2020, **22**(24), 8614–8622.

24 L.-Q. Qiu, Z.-W. Yang, X. Yao, X.-Y. Li and L.-N. He, Highly Robust Rhenium(I) Bipyridyl Complexes Containing Dipyrromethene-BF_2 Chromophores for Visible Light-Driven CO_2 Reduction, *ChemSusChem*, 2022, **15**(14), e202200337.

25 N. P. Liyanage, W. Yang, S. Guertin, S. Sinha Roy, C. A. Carpenter, R. E. Adams, R. H. Schmehl, J. H. Delcamp and J. W. Jurss, Photochemical CO_2 reduction with mononuclear and dinuclear rhenium catalysts bearing a pendant anthracene chromophore, *Chem. Commun.*, 2019, **55**(7), 993–996.

26 M. Rémond, Z. Zheng, E. Jeanneau, C. Andraud, Y. Bretonnière and S. Redon, 4,5,5-Trimethyl-2,5-dihydrofuran-Based Electron-Withdrawing Groups for NIR-Emitting Push–Pull Dipolar Fluorophores, *J. Org. Chem.*, 2019, **84**(16), 9965–9974.

27 A. Spear, R. L. Schuarca, J. Q. Bond, T. M. Korter, J. Zubieta and R. P. Doyle, Photocatalytic turnover of CO_2 under visible light by [Re$(CO)_3$(1-(1,10) phenanthroline-5-(4-nitro-naphthalimide))Cl] in tandem with the sacrificial donor BIH, *RSC Adv.*, 2022, **12**(9), 5080–5084.

28 Y. Hameed, P. Berro, B. Gabidullin and D. Richeson, An integrated Re(I) photocatalyst/sensitizer that activates the formation of formic acid from reduction of CO_2, *Chem. Commun.*, 2019, **55**(74), 11041–11044.

29 A. Nakada, K. Koike, T. Nakashima, T. Morimoto and O. Ishitani, Photocatalytic CO_2 Reduction to Formic Acid Using a Ru(II)–Re(I) Supramolecular Complex in an Aqueous Solution, *Inorg. Chem.*, 2015, **54**(4), 1800–1807.

30 K. Hirano, S. Urban, C. Wang and F. Glorius, A Modular Synthesis of Highly Substituted Imidazolium Salts, *Org. Lett.*, 2009, **11**(4), 1019–1022.

31 E. Van Den Berge and R. Robiette, Development of a Regioselective N-Methylation of (Benz)imidazoles Providing the More Sterically Hindered Isomer, *J. Org. Chem.*, 2013, **78**(23), 12220–12223.

32 K. Wang, L. Huang, L. Gao, L. Jin and C. Huang, Synthesis, Crystal Structure, and Photoelectric Properties of Re$(CO)_3$ClL (L = 2-(1-Ethylbenzimidazol-2-yl)pyridine), *Inorg. Chem.*, 2002, **41**(13), 3353–3358.

33 P. Cantero-López, Y. Hidalgo-Rosa, Z. Sandoval-Olivares, J. Santoyo-Flores, P. Mella, L. Arrué, C. Zúñiga, R. Arratia-Pérez and D. Páez-Hernández, The role of zero-field splitting and π-stacking interaction of different nitrogen-donor ligands on the optical properties of luminescent

rhenium tricarbonyl complexes, *New J. Chem.*, 2021, **45**(25), 11192–11201.

34 S. K. Pagire, N. Kumagai and M. Shibasaki, The Different Faces of $[Ru(bpy)_3Cl_2]$ and fac$[Ir(ppy)_3]$ Photocatalysts: Redox Potential Controlled Synthesis of Sulfonylated Fluorenes and Pyrroloindoles from Unactivated Olefins and Sulfonyl Chlorides, *Org. Lett.*, 2020, **22**(20), 7853–7858.

35 C. Costentin and J. M. Saveant, Homogeneous Molecular Catalysis of Electrochemical Reactions: Catalyst Benchmarking and Optimization Strategies, *J. Am. Chem. Soc.*, 2017, **139**(24), 8245–8250.

36 C. Costentin, M. Robert and J. M. Saveant, Current Issues in Molecular Catalysis Illustrated by Iron Porphyrins as Catalysts of the CO_2-to-CO Electrochemical Conversion, *Acc. Chem. Res.*, 2015, **48**(12), 2996–3006.

37 C. Costentin, G. Passard and J. M. Saveant, Benchmarking of homogeneous electrocatalysts: overpotential, turnover frequency, limiting turnover number, *J. Am. Chem. Soc.*, 2015, **137**(16), 5461–5467.

38 N. G. Connelly and W. E. Geiger, Chemical Redox Agents for Organometallic Chemistry, *Chem. Rev.*, 1996, **96**(2), 877–910.

39 B. Gholamkhass, H. Mametsuka, K. Koike, T. Tanabe, M. Furue and O. Ishitani, Architecture of Supramolecular Metal Complexes for Photocatalytic CO_2 Reduction: Ruthenium–Rhenium Bi- and Tetranuclear Complexes, *Inorg. Chem.*, 2005, **44**(7), 2326–2336.

40 R. N. Sampaio, D. C. Grills, D. E. Polyansky, D. J. Szalda and E. Fujita, Unexpected Roles of Triethanolamine in the Photochemical Reduction of CO_2 to Formate by Ruthenium Complexes, *J. Am. Chem. Soc.*, 2020, **142**(5), 2413–2428.

41 D. R. Case, A. Spear, A. F. Henwood, M. Nanao, S. Dampf, T. M. Korter, T. Gunnlaugsson, J. Zubieta and R. P. Doyle, $[Re(CO)_3(5\text{-PAN})Cl]$, a rhenium(I) naphthalimide complex for the visible light photocatalytic reduction of CO_2, *Dalton Trans.*, 2021, **50**(10), 3479–3486.

42 D. L. DuBois and D. E. Berning, Hydricity of transition-metal hydrides and its role in CO_2 reduction, *Appl. Organomet. Chem.*, 2000, **14**(12), 860–862.

43 H. Shirley, X. Su, H. Sanjanwala, K. Talukdar, J. W. Jurss and J. H. Delcamp, Durable Solar-Powered Systems with Ni-Catalysts for Conversion of CO_2 or CO to CH_4, *J. Am. Chem. Soc.*, 2019, **141**(16), 6617–6622.

44 E. G. Ha, J. A. Chang, S. M. Byun, C. Pac, D. M. Jang, J. Park and S. O. Kang, High-turnover visible-light photoreduction of CO_2 by a Re(I) complex stabilized on dye-sensitized TiO_2, *Chem. Commun.*, 2014, **50**(34), 4462–4464.

45 A. V. Müller, L. A. Faustino, K. T. de Oliveira, A. O. T. Patrocinio and A. S. Polo, Visible-Light-Driven Photocatalytic CO_2 Reduction by Re(I) Photocatalysts with N-Heterocyclic Substituents, *ACS Catal.*, 2023, **13**(1), 633–646.

46 L. Rotundo, D. C. Grills, R. Gobetto, E. Priola, C. Nervi, D. E. Polyansky and E. Fujita, Photochemical CO_2 Reduction Using Rhenium(I) Tricarbonyl Complexes with Bipyridyl-Type Ligands with and without Second Coordination Sphere Effects, *ChemPhotoChem*, 2021, **5**(6), 526–537.